16800-46-7; (B)$CrCO_3$ (B = benzene), 12082-08-5; CHT, 544-25-2; MeCHT, 4281-04-3; MeOCHT, 1714-38-1; CNCHT, 13612-59-4; *t*-BuCHT, 17635-75-5; (tropylium)chromium tricarbonyl tetrafluoroborate, 12170-19-3; (methoxytropylium)chromium tricarbonyl tetrafluoroborate, 32826-06-5; tropone, 539-80-0; dicyanocarbene, 1884-65-7; 7,7-dicyanonorcaradiene, 95388-85-5.

Supplementary Material Available: Listings of the ^{13}C and ^{1}H spectra for **9–14** and their derived rate constants (2 pages). Ordering information is given on any current masthead page.

Metal Alkoxides: Models for Metal Oxides. 8.[1] Monocarbonyl Adducts of Ditungsten Hexaalkoxides (M≡M) (RO = *t*-BuO, *i*-PrO, and *t*-$BuCH_2O$) and the Dimer $[W_2(O\text{-}i\text{-}Pr)_6(\mu\text{-}CO)]_2$

Malcolm H. Chisholm,* David M. Hoffman, and John C. Huffman

Department of Chemistry and Molecular Structure Center, Indiana University, Bloomington, Indiana 47405

Received September 6, 1984

Addition of 1 equiv of carbon monoxide to a near saturated solution of $W_2(O\text{-}t\text{-}Bu)_6$ in hexanes, with or without added pyridine (py), cooled to 0 °C leads to the precipitation of $W_2(O\text{-}t\text{-}Bu)_6(\mu\text{-}CO)$ as a red microcrystalline compound. $W_2(O\text{-}t\text{-}Bu)_6(\mu\text{-}CO)$ is isomorphous and isostructural with its molybdenum analogue and contains a central $W_2(\mu\text{-}O\text{-}t\text{-}Bu)_2(\mu\text{-}CO)$ unit: W–W = 2.526 (1) Å, W–C = 1.997 (15) Å, and C–O = 1.25 (1) Å (μ-CO). Each tungsten atom is in a square-based pyramidal geometry with the μ-CO ligand occupying the apical position. The molecule has mirror symmetry. Addition of CO (1 equiv) to hexane/pyridine solutions, ca. 6:1, of $W_2(OR)_6(py)_2$ yields under comparable conditions $W_2(OR)_6(py)_2(\mu\text{-}CO)$ compounds, where R = *i*-Pr and *t*-$BuCH_2$, as finely divided crystalline precipitates. Crystals of $W_2(O\text{-}i\text{-}Pr)_6(py)_2(CO)$ have been reexamined and shown to be identical with those previously studied (Chisholm, Huffman, Leonelli, Rothwell *J. Am. Chem. Soc.* **1982**, *104*, 7030) and have been shown to dissolve in toluene-d_8 to give $[W_2(O\text{-}i\text{-}Pr)_6(py)(\mu\text{-}CO)]_2$ and pyridine (2 equiv). This transformation appears irreversible, and all attempts to recrystallize $W_2(O\text{-}i\text{-}Pr)_6(py)_2(\mu\text{-}CO)$ yield only $[W_2(O\text{-}i\text{-}Pr)_6(py)(\mu\text{-}CO)]_2$, previously characterized by Cotton and Schwotzer (*J. Am. Chem. Soc.* **1983**, *105*, 4955). Solution ^{1}H and ^{13}C NMR and IR spectral data indicate that $W_2(OCH_2\text{-}t\text{-}Bu)_6(py)_2(\mu\text{-}CO)$ is present in hydrocarbon solutions, while addition of *i*-PrOH (>6 equiv) to $W_2(O\text{-}t\text{-}Bu)_6(\mu\text{-}CO)$ yields $[W_2(O\text{-}i\text{-}Pr)_6(\mu\text{-}CO)]_2$, which is closely related to the Cotton and Schwotzer pyridine adduct. These findings are understandable in terms of steric control in the binding of pyridine to the ditungsten center and the nucleophilic properties of the $W_2(\mu\text{-}CO)$ oxygen atom. In the solid state, molecules of $[W_2(O\text{-}i\text{-}Pr)_6(\mu\text{-}CO)]_2$ are centrosymmetric and contain an essentially planar central $[W_2(\mu\text{-}CO)]_2$ unit with W–W = 2.657 (1) Å, W–C = 1.95 (1) Å (averaged), W–O = 1.97 (1) Å, and C–O = 1.35 (1) Å. Each tungsten atom is in a distorted trigonal-bipyramidal environment and NMR studies show that, while the central $[W_2(\mu\text{-}CO)]_2$ unit is rigid on the NMR time scale, scrambling of the terminal OR ligands occurs at two of the symmetry-related tungsten atoms. The reaction sequence W≡W + C≡O → $W_2(\mu\text{-}CO)$ → $[W_2(\mu\text{-}CO)]_2$ represents a stepwise reduction in M–M and C–O bond order from 3 to 2 to 1 and is suggestive of a model for the reaction pathway of C≡O on a metal oxide leading untimately to carbide, C^{4-}, and oxide, O^{2-}. Differences in the binding of CO to the $(W{\equiv}W)^{6+}$ and $(Mo{\equiv}Mo)^{6+}$ units in $M_2(OR)_6$ compounds are related to the greater reducing power (π-back-bonding) of the ditungsten center. Crystal data for $W_2(O\text{-}t\text{-}Bu)_6(\mu\text{-}CO)$ at −162 °C: a = 17.660 (2) Å, b = 9.182 (13) Å, c = 19.307 (5) Å, Z = 4, and space group $Cmc2_1$. Crystal data for $[W_2(O\text{-}i\text{-}Pr)_6(\mu\text{-}CO)]_2$ at −162 °C: a = 12.085 (2) Å, b = 17.224 (4) Å, c = 13.027 (3) Å, β = 99.25 (1)°, Z = 2, and space group $P2_1/n$.

Introduction

Kelly[2] first discovered that hydrocarbon solutions of $Mo_2(O\text{-}t\text{-}Bu)_6$ and C≡O react rapidly at room temperature and 1 atm according to the stoichiometry shown in eq 1.

$$2Mo_2(O\text{-}t\text{-}Bu)_6 + 6CO \rightarrow Mo(CO)_6 + 3Mo(O\text{-}t\text{-}Bu)_4 \quad (1)$$

The first step in (1) is the reversible formation of $Mo_2(O\text{-}t\text{-}Bu)_6(\mu\text{-}CO)$, I. Carbonylation of $Mo_2(O\text{-}i\text{-}Pr)_6$ proceeds similarly to give $Mo(CO)_6$, and in the presence of pyridine an initial carbonyl adduct, $Mo_2(O\text{-}i\text{-}Pr)_6(py)_2(\mu\text{-}CO)$, has been isolated and characterized.[3] The latter compound adopts the structure shown in II which is closely related to I having Mo–N bonds trans to the Mo–C bond, thereby completing octahedral coordination of each molybdenum atom.

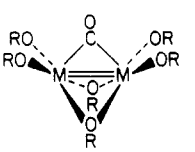

I, M=Mo or W, R=*t*-Bu

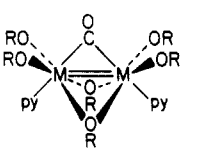

II, M=Mo or W, R=*i*-Pr or CH_2-*t*-Bu

In the case of the carbonylation of $Mo_2(O\text{-}i\text{-}Pr)_6$, the oxidized form of molybdenum is $Mo_2(O\text{-}i\text{-}Pr)_8(CO)_2$ which is believed to have the edge-shared bioctahedral structure shown in III.[4]

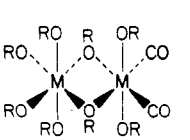

III, M=Mo, R=*i*-Pr

(1) Part 7. Chisholm, M. H.; Folting, K.; Heppert, J. A.; Hoffman, D. M.; Huffman, J. C. *J. Am. Chem. Soc.* **1985**, *107*, 1234.
(2) Chisholm, M. H.; Cotton, F. A.; Extine, M. W.; Kelly, R. L. *J. Am. Chem. Soc.* **1979**, *101*, 7645.
(3) Chisholm, M. H.; Huffman, J. C.; Leonelli, J.; Rothwell, I. P. *J. Am. Chem. Soc.* **1982**, *104*, 7030.
(4) Chisholm, M. H.; Huffman, J. C.; Kelly, R. L. *J. Am. Chem. Soc.* **1979**, *101*, 7615.

0276-7333/85/2304-0986$01.50/0 © 1985 American Chemical Society

Carbonylation of $W_2(OR)_6$ or $W_2(OR)_6(py)_2$ compounds also leads to $W(CO)_6$ under very mild conditions, and we were able to isolate a tungsten analogue of II.[3] However, the details of the reaction pathways differ for the two metals in a number of interesting ways, one of which is that CO induces a cleavage of the $(W{\equiv}W)^{6+}$ unit by disproportionation to W(0) and W(6+) in the case of R = *i*-Pr. Cotton and Schwotzer[5] isolated a compound of formula $W_2(O\text{-}i\text{-}Pr)_6(CO)_4$ during their studies of the reaction between $W_2(O\text{-}i\text{-}Pr)_6$ and CO. The structure of this interesting molecule, depicted by IV below, contains a very asymmetrically bound pair of μ-OR bridges implying that a $W(O\text{-}i\text{-}Pr)_6$ molecule is ligated to a $W(CO)_4$ fragment.

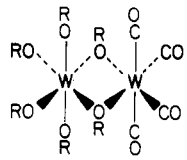

IV, R = *i*-Pr

The stepwise conversion of an unbridged $(RO)_3M{\equiv}M(OR)_3$ compound to $M(CO)_6$ by successive CO uptake and CO/OR terminal $\rightleftharpoons$ bridge migrations via intermediates of type I, II, III, and IV is easily envisaged.

The compounds I and II show very low carbonyl stretching frequencies for μ-CO ligands, e.g., ν(CO) 1655 and 1575 cm^{-1} in II where M = Mo and W, respectively. Typical values of ν(CO) for μ-CO ligands in neutral molecules fall within the range 1700–1860 cm^{-1}. We suggested that the low values of ν(CO) in compounds II could be understood in terms of the resonance structures shown in Va–c. This led us to predict that the oxygen atoms of the $M_2(\mu\text{-CO})$ moiety should be nucleophilic and would associate with other Lewis acidic metal centers.[3]

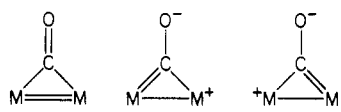

Va Vb Vc

It was therefore of considerable interest to us to learn that Cotton and Schwotzer in their study of the reaction between $W_2(O\text{-}i\text{-}Pr)_6(py)_2$ and CO were not able to verify the formation of $W_2(O\text{-}i\text{-}Pr)_6(py)_2(\mu\text{-CO})$. Instead they isolated and characterized a tetranuclear molecule $[W_2(O\text{-}i\text{-}Pr)_6(py)(\mu\text{-CO})]_2$ having the structure depicted by VI below.[6]

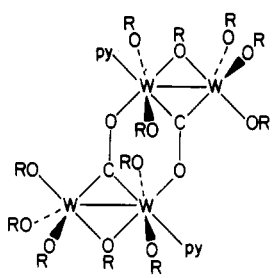

VI

A consideration of the distances associated with the central $[W_2(\mu\text{-CO})]_2$ unit led Cotton and Schwotzer[6] to depict VI in terms of the VB structures shown in VIIa and VIIb. These can be seen to arise by the dimerization of Vb and Vc, respectively.

The formation of $[W_2(O\text{-}i\text{-}Pr)_6(py)(CO)]_2$ from $W_2(O\text{-}i\text{-}Pr)_6(py)_2(CO)$ by loss of pyridine and the reverse reaction

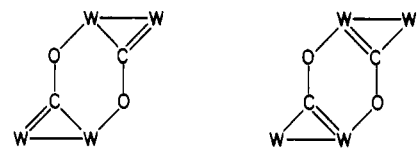

VIIa VIIb

involving the cleavage of the tetranuclear compound to give two $W_2(\mu\text{-CO})$ containing compounds can be envisaged as an equilibrium (eq 2).

$$2W_2(O\text{-}i\text{-}Pr)_6(py)_2(\mu\text{-CO}) \rightleftharpoons [W_2(O\text{-}i\text{-}Pr)_6(py)(\mu\text{-CO})]_2 + 2py \quad (2)$$

The characterization of the $[W_2(O\text{-}i\text{-}Pr)_6(py)(\mu\text{-CO})]_2$ molecule cast doubt concerning the existence of $W_2(O\text{-}i\text{-}Pr)_6(py)_2(\mu\text{-CO})$ in solution and Cotton and Schwotzer[6] wrote: "It seems likely, therefore, that the predominant species in solution is, in both cases, the tetranuclear species and that the following equilibrium (eq 2, shown above) prevails."

We determined to investigate these matters further and report here our findings concerning the formation and properties of monocarbonyl adducts of ditungsten hexaalkoxides where RO = *t*-BuO, *i*-Pr, and *t*-$BuCH_2O$.

Results and Discussion

Synthesis and Physicochemical Properties. $W_2(O\text{-}t\text{-}Bu)_6(\mu\text{-CO})$ and $W_2(OR)_6(py)_2(\mu\text{-CO})$, Where R = *i*-Pr or *t*-$BuCH_2$. A common procedure was used to prepare the carbonyl-bridged dinuclear compounds. The addition of 1 equiv of carbon monoxide to a concentrated solution (nearly saturated) of $W_2(O\text{-}t\text{-}Bu)_6$ or $W_2(OR_6(py)_2$ in hexane or hexane/pyridine at 0 °C led to an immediate reaction and the formation of microcrystalline precipitates of the compounds $W_2(O\text{-}t\text{-}Bu)_6(\mu\text{-CO})$ or $W_2(OR)_6(py)_2(\mu\text{-CO})$, where R = *i*-Pr or *t*-$BuCH_2$. The precipitates were collected by filtration and dried under vacuum. Isolated yields range from 60 to 85% based on the theoretical for 1:1 adduct formation. We believe the yields are controlled by the relative solubilities of the compounds and some mechanical loss due to the handling of relatively small samples by Schlenk and drybox techniques.

The compounds are air sensitive and must be handled under dry and oxygen-free atmospheres (N_2). They show a very characteristic strong band or bands in the infrared spectra in the range 1600–1560 cm^{-1} assignable to the bridging carbonyl ligand. IR spectra recorded as Nujol mulls sometimes showed more than one band in this region, as noted in Table I. This we believe to be due to solid-state effects since in solution only one band is observed.

The compound $W_2(O\text{-}t\text{-}Bu)_6(\mu\text{-CO})$ is notably more stable than its molybdenum analogue, I, which reversibly loses CO and reacts further with CO leading to its decomposition according to eq 3.[2]

$$6Mo_2(O\text{-}t\text{-}Bu)_6(\mu\text{-CO}) \rightarrow 4Mo_2(O\text{-}t\text{-}Bu)_6 + Mo(CO)_6 + 3Mo(O\text{-}t\text{-}Bu)_4 \quad (3)$$

Reaction 3 has a half-life of the order of 1 h at room temperature, and applying a dynamic vacuum or N_2 flush readily drives off CO with the regeneration of $Mo_2(O\text{-}t\text{-}Bu)_6$. By contrast $W_2(O\text{-}t\text{-}Bu)_6(\mu\text{-CO})$ is stable in solution at room temperature for several hours and can be recrystallized after heating the solution to 50 °C. Over a period of days/weeks decomposition does occur, but only a very small amount of the CO ligand ends up as $W(CO)_6$ as judged by IR and ^{13}C NMR spectroscopy. It is not known what the decomposition products are, and this remains an area for future investigations.

(5) Cotton, F. A.; Schwotzer, W. *J. Am. Chem. Soc.* **1983**, *105*, 5639.
(6) Cotton, F. A.; Schwotzer, W. *J. Am. Chem. Soc.* **1983**, *105*, 4955.

Table I. Pertinent Infrared and ^{13}C NMR Data for the $M_2(\mu\text{-CO})$ and $[W_2(\mu\text{-CO})]_2$ Containing Compounds and Related Molybdenum Compounds

compound	ν_{CO},[a] cm^{-1}	ν^{13}_{CO}, cm^{-1}	$\delta(^{13}CO)$[b]	$^1J_{^{183}W-^{13}C}$, Hz	^{13}C NMR temp/sol	ref
$W_2(O\text{-}t\text{-}Bu)_6(\mu\text{-CO})$	1598 (1605)[c]	1559	291.0	192.9	21 °C/C_6D_6	*h*
$Mo_2(O\text{-}t\text{-}Bu)_6(\mu\text{-CO})$	1670	NR[d]	272.5		21 °C/C_6D_6	*i*
$W_2(OCH_2\text{-}t\text{-}Bu)_6(py)_2(\mu\text{-CO})$	1587 1579 1567 (1595)[c]	1546 1538 (1570)[c]	321.6	150.3	−60 °C/C_7D_8	*h*
$Mo_2(OCH_2\text{-}t\text{-}Bu)_6(py)_2(\mu\text{-CO})$	1660	NR	323.6		20 °C/C_6D_6	*j*
$W_2(O\text{-}i\text{-}Pr)_6(py)_2(\mu\text{-CO})$	1570 1579 (1298)[c]	1533 (1271)[c]	341[e]			*h*
$Mo_2(O\text{-}i\text{-}Pr)_6(py)_2(\mu\text{-CO})$	1655	1618	331.5		25 °C/C_6D_6	*j*
$[W_2(O\text{-}i\text{-}Pr)_6(\mu\text{-CO})]_2$	1272	1243	305.5	188.9[f] 164.0	−55 °C/C_7D_8	*h*
$[W_2(O\text{-}i\text{-}Pr)_6(py)(\mu\text{-CO})]_2$	1305 (1298)[c]	1265	310.4	170.0[g]	34 °C/C_7D_8	*h* (IR), *j*, *k* (NMR)

[a] IR spectra were recorded for Nujol mulls between CsI plates except when noted. [b] In ppm relative to Me_4Si. [c] IR spectrum recorded for a toluene solution. [d] NR = not reported. [e] Magic-angle ^{13}C NMR value. We acknowledge Dr. J. P. Yesinowski and the use of the Southern California Regional NMR facility supported by NSF Grant CHE 79-16324 for obtaining this data. Solution value from footnote *j* below is incorrect. [f] Consistent with the solid-state structure, there are two $^{183}W-^{13}C$ coupling constants. [g] Only one $^{183}W-^{13}C$ coupling constant reported. [h] This work. [i] Reference 2. [j] Reference 3. [k] Reference 6.

The formation of $W_2(O\text{-}i\text{-}Pr)_6(py)_2(\mu\text{-CO})$ was confirmed by an examination of the crystals initially formed from hexane/pyridine solutions. These were found to have the same space group and cell dimensions as those reported previously.[3] The bulk samples are believed to be $W_2(O\text{-}i\text{-}Pr)_6(py)_2(\mu\text{-CO})$ on the basis of their IR spectra which are identical with those obtained from crystalline samples. We cannot rule out, however, that in the finely divided precipitates there are some contaminants such as $[W_2(O\text{-}i\text{-}Pr)_6(py)(\mu\text{-CO})]_2$.

When freshly prepared $W_2(O\text{-}i\text{-}Pr)_6(py)_2(\mu\text{-CO})$ is dissolved in toluene or benzene, crystallization yields only the red crystalline compound $[W_2(O\text{-}i\text{-}Pr)_6(py)(\mu\text{-CO})]_2$. This was determined by examination of the crystals which were found to have the same space group and unit cell dimensions as those reported by Cotton and Schwotzer.[6] The ^{13}C NMR spectra also agreed with that reported by those authors.

We conclude that what went into solution did not come out of solution. This still leaves the question: what was in solution?

Solution infrared spectra recorded on a freshly prepared sample of $W_2(O\text{-}i\text{-}Pr)_6(py)_2(\mu\text{-CO})$ dissolved in toluene did not show any band at ca. 1570 cm^{-1} assignable to the $W_2(\mu\text{-CO})$ moiety. The variable-temperature ^1H NMR spectra recorded in toluene-d_8 are entirely consistent with the presence of $[W_2(O\text{-}i\text{-}Pr)_6(py)(\mu\text{-CO})]_2$ and free pyridine. The addition of more pyridine does not affect the low-temperature limiting ^1H NMR spectrum of the tungsten complex nor does it produce a band at ca. 1570 cm^{-1} in the IR spectrum.

The compound $W_2(OCH_2\text{-}t\text{-}Bu)_6(py)_2(\mu\text{-CO})$ does show a solution IR band at 1595 cm^- and its low-temperature limiting ^1H NMR spectrum is consistent with expectations based on the adoption of a structure of type II. The compound is, however, not indefinitely stable in solution and like the *tert*-butoxide decomposes over a period of days/weeks to as yet unidentified compounds of which $W(CO)_6$ is a very minor component.

$[W_2(O\text{-}i\text{-}Pr)_6(\mu\text{-CO})]_2$ is best prepared by the addition of *i*-PrOH (>6 equiv) to a hexane solution of $W_2(O\text{-}t\text{-}Bu)_6(\mu\text{-CO})$. The yield obtained by crystallization from hexane was 65%, and examination of the ^1H NMR spectrum of the solids obtained by stripping the filtrate showed that this was mostly $[W_2(O\text{-}i\text{-}Pr)_6(\mu\text{-CO})]_2$.

Table II. Fractional Coordinates and Isotropic Thermal Parameters for the $W_2(O\text{-}t\text{-}Bu)_6(\mu\text{-CO})$ Molecule[a]

atom	10^4x	10^4y	10^4z	$10B_{iso}$, Å^2
W(1)	9284.9 (2)	7259.1 (4)	7500*	11
O(1)	10000*	4321 (14)	7123 (8)	22
O(2)	10000*	8050 (16)	8283 (8)	14
O(3)	10000*	8780 (16)	7040 (7)	11
O(4)	8605 (6)	7192 (12)	6770 (6)	18
O(5)	8642 (6)	6397 (12)	8167 (5)	17
C(1)	10000*	5636 (21)	7286 (9)	12
C(2)	10000*	8483 (23)	8997 (11)	21 (4)
C(3)	10000*	7183 (28)	9459 (14)	35 (5)
C(4)	9305 (11)	9373 (28)	9160 (13)	52 (5)
C(5)	10000*	10386 (21)	6987 (10)	14 (3)
C(6)	10000*	10732 (42)	6248 (18)	63 (8)
C(7)	10688 (9)	10936 (21)	7320 (9)	37 (4)
C(8)	8425 (9)	6731 (17)	6072 (8)	25 (3)
C(9)	8792 (10)	5316 (20)	5929 (10)	39 (4)
C(10)	7578 (12)	6578 (23)	6044 (10)	43 (4)
C(11)	8686 (12)	7909 (21)	5594 (11)	40 (4)
C(12)	8291 (7)	5078 (16)	8425 (8)	18 (3)
C(13)	7795 (10)	5537 (19)	9029 (9)	31 (3)
C(14)	7814 (9)	4443 (18)	7846 (8)	29 (3)
C(15)	8895 (9)	4017 (18)	8646 (9)	29 (3)

[a] Parameters marked by asterisk (*) were not varied.

It is of interest to note that the addition of CO (1 equiv) to a hydrocarbon solution of $W_2(O\text{-}i\text{-}Pr)_6(PMe_3)_2$ also led to the isolation of $[W_2(O\text{-}i\text{-}Pr)_6(\mu\text{-CO})]_2$ as the only crystallizable product from hexane, though the isolated yield was lower, 26%.

Solid-State and Molecular Structures. $W_2(O\text{-}t\text{-}Bu)_6(\mu\text{-CO})$ crystallizes from toluene in the space group *Cmc*2, and is isomorphous and isostructural with its molybdenum analogue I[2] and has crystallographically imposed mirror symmetry. Atomic positional parameters are given in Table II, and an ORTEP view of the molecule showing the atom numbering scheme is given in Figure 1. Selected bond distances with a comparison with those of the molybdenum analogue I are given in Table III. Selected bond angles for the tungsten compound are given in Table IV.

The two compounds are, not surprisingly, very similar in the details of their structure. The metal–oxygen bond distances are essentially identical. The W–W distance is longer by 0.028 (1) Å while for the $M_2(\mu\text{-CO})$ moiety the M–C and C–O distances appear shorter and longer, respectively, in the tungsten compound than they do in the

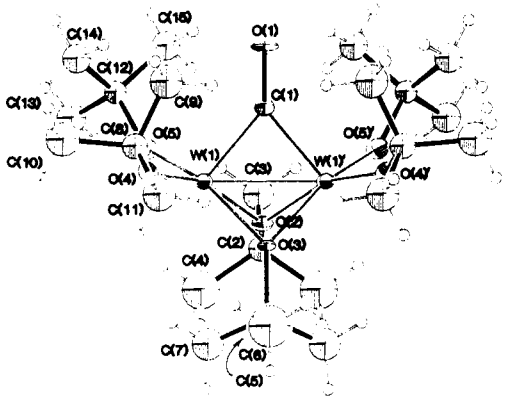

Figure 1. An ORTEP view of the $W_2(O\text{-}t\text{-}Bu)_6(\mu\text{-}CO)$ molecule giving the atom numbering scheme used in the tables. The molecule has crystallographically imposed mirror symmetry.

Table III. Comparison of Pertinent Distances (Å) in the $M_2(O\text{-}t\text{-}Bu)_6(\mu\text{-}CO)$ Molecules

		distances	
A	B	M = W	M = Mo[2]
M(1)	M(1)′	2.5257 (8)	2.489 (1)
M(1)	O(2)	2.099 (11)	2.093 (8)
M(1)	O(3)	2.082 (10)	2.074 (8)
M(1)	O(4)	1.852 (11)	1.888 (7)
M(1)	O(5)	1.890 (10)	1.876 (8)
M(1)	C(1)	1.997 (15)	2.022 (10)
O(1)	C(1)	1.247 (23)	1.21 (2)
O(2)	C(2)	1.435 (26)	1.39 (2)
O(3)	C(5)	1.478 (25)	1.45 (2)
O(4)	C(8)	1.449 (19)	1.43 (2)
O(5)	C(12)	1.448 (18)	1.43 (1)
C	C(methyl)	1.50	

Table IV. Selected Bond Angles (deg) for the $W_2(O\text{-}t\text{-}Bu)_6(\mu\text{-}CO)$ Molecule

A	B	C	angle
W(1)	W(1)	O(2)	53.02 (22)
W(1)	W(1)	O(3)	52.66 (22)
W(1)	W(1)	O(4)	130.4 (3)
W(1)	W(1)	O(5)	126.9 (3)
W(1)	W(1)	C(1)	50.8 (3)
O(2)	W(1)	O(3)	73.2 (6)
O(2)	W(1)	O(4)	161.7 (5)
O(2)	W(1)	O(5)	90.9 (5)
O(2)	W(1)	C(1)	91.5 (5)
O(3)	W(1)	O(4)	95.2 (5)
O(3)	W(1)	O(5)	159.4 (5)
O(3)	W(1)	C(1)	91.6 (5)
O(4)	W(1)	O(5)	96.6 (4)
O(4)	W(1)	C(1)	103.2 (5)
O(5)	W(1)	C(1)	102.0 (6)
W(1)	O(2)	W(1)	74.0 (4)
W(1)	O(2)	C(2)	142.0 (4)
W(1)	O(3)	W(1)	74.7 (4)
W(1)	O(3)	C(5)	134.3 (7)
W(1)	O(4)	C(8)	149.3 (10)
W(1)	O(5)	C(12)	147.2 (9)
W(1)	C(1)	W(1)	78.5 (7)
W(1)	C(1)	O(1)	140.8 (3)
O(2)	C(2)	C(3)	110.7 (18)
O(2)	C(2)	C(4)	110.5 (14)
O(3)	C(5)	C(6)	106.5 (21)
O(3)	C(5)	C(7)	108.3 (12)
O(4)	C(8)	C(9)	109.6 (13)
O(4)	C(8)	C(10)	106.2 (13)
O(4)	C(8)	C(11)	107.2 (13)
O(5)	C(12)	C(13)	106.2 (12)
O(5)	C(12)	C(14)	107.8 (12)
O(5)	C(12)	C(15)	109.6 (11)

molybdenum compound. The precision of the M–C and C–O distances is not sufficient to say more than this is an apparent trend. It is, of course, just the trend we would expect and would account for the greater degree of W-to-C–O π-back-bonding as evidenced by the lower ν(CO) value relative to I, M = Mo.

Table V. Fractional Coordinates and Isotropic Thermal Parameters for the $[W_2(O\text{-}i\text{-}Pr)_6(\mu\text{-}CO)]_2$ Molecule

atom	10^4x	10^4y	10^4z	$10B_{iso}$, Å^2
W(1)	4003.0 (4)	3804.4 (3)	2972.8 (3)	16
W(2)	5862.8 (4)	4449.4 (3)	3980.4 (3)	16
O(1)	6293 (6)	5175 (5)	5150 (6)	24
O(2)	5653 (6)	3775 (4)	2706 (5)	15
O(3)	2419 (6)	3816 (4)	2921 (6)	22
O(4)	4166 (6)	2753 (4)	3347 (6)	23
O(5)	3798 (7)	4317 (5)	1648 (6)	26
O(6)	6637 (7)	3666 (5)	4804 (6)	28
O(7)	6149 (6)	5266 (4)	3107 (6)	23
C(1)	4302 (9)	4473 (6)	4188 (7)	15
C(2)	6185 (11)	3770 (7)	1794 (9)	27
C(3)	5686 (13)	3116 (7)	1096 (10)	37
C(4)	7434 (10)	3714 (8)	2142 (10)	33
C(5)	1609 (9)	3934 (7)	3563 (9)	22
C(6)	648 (12)	4389 (9)	3007 (14)	49
C(7)	1263 (14)	3179 (10)	3908 (15)	57
C(8)	4877 (9)	2243 (7)	4032 (10)	25
C(9)	4795 (11)	1440 (7)	3540 (11)	36
C(10)	4519 (13)	2248 (8)	5078 (11)	42
C(11)	2972 (11)	4850 (10)	1150 (12)	45
C(12)	3390 (16)	5646 (10)	1275 (15)	62
C(13)	2705 (21)	4585 (14)	55 (17)	98
C(14)	7495 (10)	3625 (9)	5697 (10)	34
C(15)	8611 (12)	3665 (12)	5345 (13)	58
C(16)	7307 (15)	2906 (10)	6269 (13)	60
C(17)	6690 (11)	6001 (8)	3256 (10)	33
C(18)	7899 (15)	5890 (13)	3165 (19)	84
C(19)	6117 (20)	6568 (9)	2466 (15)	75

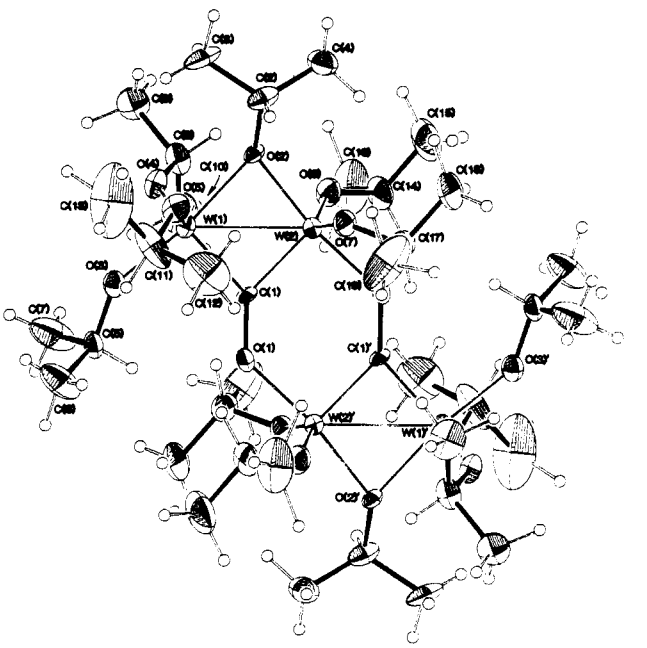

Figure 2. An ORTEP view of the centrosymmetric $[W_2(O\text{-}i\text{-}Pr)_6(\mu\text{-}CO)]_2$ molecule giving the atom numbering scheme used in the Tables.

$[W_2(O\text{-}i\text{-}Pr)_6(\mu\text{-}CO)]_2$. In the space group $P2_1/n$ molecules of $[W_2(O\text{-}i\text{-}Pr)_6(\mu\text{-}CO)]_2$ have a crystallographically imposed center of symmetry. Atomic positional parameters are given in Table V, and an ORTEP view of the molecule giving the atom numbering system is given in Figure 2. Selected bond distances and angles are given in Table VI.

A ball and stick drawing of the central $[W_2(\mu\text{-}CO)O_6]_2$ skeleton of the molecule is given in Figure 3. Each tungsten atom is in a trigonalbipyramidal environment in

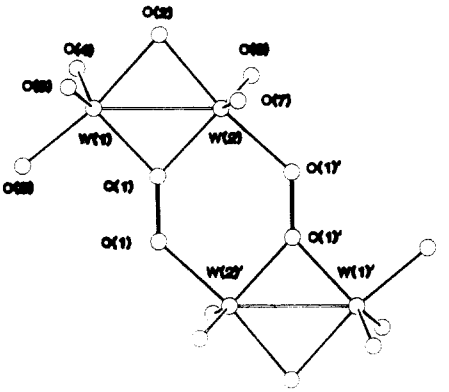

Figure 3. A ball and stick drawing of the central $[W_2(\mu\text{-}CO)O_6]_2$ skeleton of the $[W_2(O\text{-}i\text{-}Pr)_6(\mu\text{-}CO)]_2$ molecule showing the trigonal-bipyramidal coordination of each tungsten atom.

which the W–C bonds occupy equatorial positions.

The W–W distance, 2.657 (1) Å, is typical of a W–W single bond distance,[7] and the C–O distance of the μ-CO ligand, 1.35 (1) Å, is typical of a C_{sp^3}–O single bond distance.[8] The W–O distance of the $[W_2(\mu\text{-}CO)]_2$ moiety, 1.97 (1) Å, falls in a range commonly observed for Mo–OR or W–OR distances where some O-to-M π-bonding is involved.[7] It is, however, somewhat longer than the W–O distances seen for the terminal W–OR bonds in this molecule, the maximum difference being 0.1 Å, but it is shorter than those generally seen for bridging OR ligands which are typically close to 2.06 Å.[7] The latter can be taken as approaching a pure σ-bond M–OR distance. The W–C distance 1.95 (1) Å is shorter than that seen in compounds of type I and II. All these changes are consistent with the depiction of the bonding in the central $[W_2(\mu\text{-}CO)]_2$ by VIIa and VIIb. The central $[W_2(\mu\text{-}CO)]_2$ unit is essentially planar with none of the six atoms deviating by more than 0.022 Å from an idealized plane.

The $[W_2(O\text{-}i\text{-}Pr)_6(\mu\text{-}CO)]_2$ molecule is, as expected, very similar to the pyridine adduct $[W_2(O\text{-}i\text{-}Pr)_6(py)(\mu\text{-}CO)]_2$ characterized by Cotton and Schwotzer.[6] The pyridine ligands coordinate to a pair of symmetry related tungsten atoms W(2) and W(2)′ with remarkably little effect on the other metal–ligand bonds and ligand conformations. This is probably best demonstrated by the superposition of the molecules as shown in the supplementary material.

IR and NMR Studies. Selected IR and ^{13}C NMR data for the new compounds along with related compounds are given in Table I.

Carbonyl-Bridged Dinuclear Compounds. As noted earlier in this paper a characteristic of the $W_2(\mu\text{-}CO)$ moiety is the appearance of an IR band or bands in the region 1600–1560 cm^{-1}. These bands are 70–80 cm^{-1} lower in energy than those found in molybdenum analogues. This is an indication of the better π-back-bonding between W and the empty CO π^*-orbitals. This trend parallels the values of ν(NO) in compounds of formula $M(OR)_3(NO)L$ where L = a neutral donor ligand or an alkoxide bridge: ν(NO) ca. 1640 cm^{-1} for M = Mo and ca. 1550 cm^{-1} for M = W.[9] These differences can be explained in terms of the relative screening of the valence electrons by the inner-core electrons. For compounds of molybdenum or tungsten in their middle to higher oxidation state, the extra 32 core electrons that are present for tungsten will screen the valence electrons from the effective higher atomic charge.

Table VI. Selected Bond Distances (Å) and Angles (deg) for the $[W_2(O\text{-}i\text{-}Pr)_6(\mu\text{-}CO)]_2$ Molecule

A	B	dist	A	B	dist
W(1)	W(2)	2.6572 (13)	O(5)	C(11)	1.433 (16)
W(1)	O(2)	2.079 (7)	O(6)	C(14)	1.430 (14)
W(1)	O(3)	1.905 (8)	O(7)	C(17)	1.423 (15)
W(1)	O(4)	1.878 (8)	C(2)	C(3)	1.511 (19)
W(1)	O(5)	1.919 (8)	C(2)	C(4)	1.508 (19)
W(1)	C(1)	1.945 (10)	C(5)	C(6)	1.488 (20)
W(2)	O(1)	1.974 (8)	C(5)	C(7)	1.460 (23)
W(2)	O(2)	2.009 (7)	C(8)	C(9)	1.521 (20)
W(2)	O(6)	1.878 (8)	C(8)	C(10)	1.494 (21)
W(2)	O(7)	1.876 (8)	C(11)	C(12)	1.460 (27)
W(2)	C(1)	1.949 (11)	C(11)	C(13)	1.48 (4)
O(1)	C(1)	1.352 (13)	C(14)	C(15)	1.494 (22)
O(2)	C(2)	1.439 (14)	C(14)	C(16)	1.482 (23)
O(3)	C(5)	1.401 (14)	C(17)	C(18)	1.498 (26)
O(4)	C(8)	1.434 (14)	C(17)	C(19)	1.505 (28)

A	B	C	angle	A	B	C	angle
W(2)	W(1)	O(2)	48.32 (18)	O(6)	W(2)	O(7)	139.6 (4)
W(2)	W(1)	O(3)	141.16 (24)	O(6)	W(2)	C(1)	109.9 (4)
W(2)	W(1)	O(4)	103.30 (23)	O(7)	W(2)	C(1)	110.2 (4)
W(2)	W(1)	O(5)	103.21 (25)	W(2)	O(1)	C(1)	132.4 (7)
W(2)	W(1)	C(1)	47.0 (3)	W(1)	O(2)	W(2)	81.08 (25)
O(2)	W(1)	O(3)	168.4 (3)	W(1)	O(2)	C(2)	134.9 (7)
O(2)	W(1)	O(4)	87.5 (3)	W(2)	O(2)	C(2)	132.2 (7)
O(2)	W(1)	O(5)	81.3 (3)	W(1)	O(3)	C(5)	140.8 (7)
O(2)	W(1)	C(1)	9k.3 (4)	W(1)	O(4)	C(8)	141.1 (7)
O(3)	W(1)	O(4)	94.7 (3)	W(1)	O(5)	C(11)	133.0 (8)
O(3)	W(1)	O(5)	88.8 (3)	W(2)	O(6)	C(14)	136.8 (8)
O(3)	W(1)	C(1)	94.4 (4)	W(2)	O(7)	C(17)	135.1 (8)
O(4)	W(1)	O(5)	132.1 (3)	W(1)	C(1)	W(2)	86.1 (4)
O(4)	W(1)	C(1)	111.2 (4)	W(1)	C(1)	O(1)	137.5 (8)
O(5)	W(1)	C(1)	116.1 (4)	W(2)	C(1)	O(1)	136.4 (8)
W(1)	W(2)	O(1)	137.97 (22)	O(2)	C(2)	C(3)	108.2 (11)
W(1)	W(2)	O(2)	50.60 (20)	O(2)	C(2)	C(4)	108.1 (10)
W(1)	W(2)	O(6)	106.62 (25)	O(3)	C(5)	C(6)	110.6 (12)
W(1)	W(2)	O(7)	103.73 (24)	O(3)	C(5)	C(7)	108.4 (12)
W(1)	W(2)	C(1)	46.9 (3)	O(4)	C(8)	C(9)	107.6 (11)
O(1)	W(2)	O(2)	170.6 (3)	O(4)	C(8)	C(10)	109.4 (11)
O(1)	W(2)	O(6)	88.2 (4)	O(5)	C(11)	C(12)	110.4 (13)
O(1)	W(2)	O(7)	86.7 (3)	O(5)	C(11)	C(13)	105.4 (19)
O(1)	W(2)	C(1)	91.2 (4)	O(6)	C(14)	C(15)	108.6 (12)
O(2)	W(2)	O(6)	92.4 (3)	O(6)	C(14)	C(16)	107.5 (12)
O(2)	W(2)	O(7)	86.8 (3)	O(7)	C(17)	C(18)	108.0 (15)
O(2)	W(2)	C(1)	97.5 (4)	O(7)	C(17)	C(19)	109.4 (14)

Thus, in terms of an orbital energy match and radial extension, tungsten's valence d orbitals will be better suited for π-back-bonding to the vacant high energy CO π^*-orbitals than will molybdenum's valence orbitals.

The ^1H NMR spectra recorded in toluene-d_8, 360 MHz in the temperature range −95 to +22 °C, showed only a single signal for the 54 protons in $W_2(O\text{-}t\text{-}Bu)_6(\mu\text{-}CO)$. Like its molybdenum analogue I, bridge ⇌ terminal OR exchange is very facile.

In contrast, low-temperature limiting ^1H and ^{13}C NMR spectra were obtained for $W_2(OCH_2\text{-}t\text{-}Bu)_6(py)_2(\mu\text{-}CO)$. The ^1H NMR spectrum recorded at −60 °C shows the neopentoxy ligands give rise to two singlets (36 H and 18 H) in the t-Bu region and a singlet (4 H) and an AB quartet (8H) in the methylene region. In addition resonances are observed for coordinated pyridine. The $^{13}C\{^1H\}$ NMR spectrum recorded at −60 °C reveals six carbon resonances for the neopentoxy ligands (two for the methyl carbon atoms, two for the tertiary carbon atoms, and two for the methylene carbon atoms). Collectively, the ^1H and ^{13}C NMR data are fully consistent with the confacial bioctahedral structure represented by II.

$[W_2(\mu\text{-}CO)]_2$-Containing Compounds. As noted previously in this paper, the infrared spectra obtained on samples of $W_2(O\text{-}i\text{-}Pr)_6(py)_2(\mu\text{-}CO)$ dissolved in toluene do not show evidence of the $W_2(\mu\text{-}CO)$ group. The ^1H and ^{13}C NMR spectra recorded in toluene-d_8 of "$W_2(O\text{-}i\text{-}$

(7) Chisholm, M. H. *Polyhedron* **1983**, *2*, 681.
(8) Kitchitsu, K. *MTP Int. Rev. Sci.; Phys. Chem., Ser. One* **1972**, *11*, 221.
(9) Chisholm, M. H.; Cotton, F. A.; Extine, M. W.; Kelly, R. L. *Inorg. Chem.* **1979**, *18*, 116.

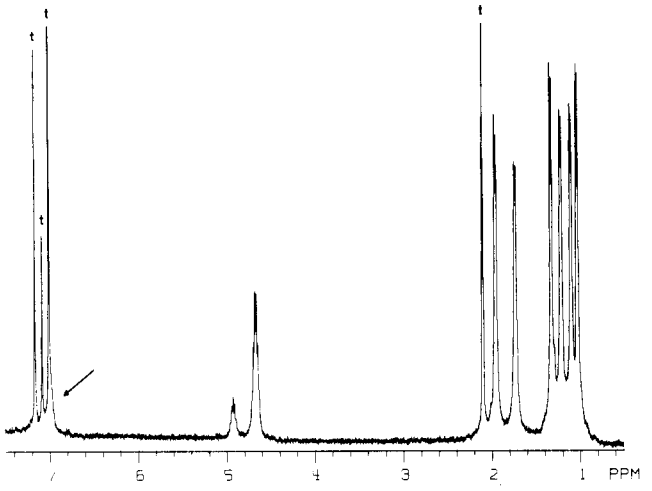

Figure 4. ^{1}H NMR spectrum of a sample of $[W_2(O\text{-}i\text{-}Pr)_6(\mu\text{-}CO)]_2$ dissolved in toluene-d_8 recorded at 360 MHz and −75 °C. The signals indicated by "t" arise from the residual protons in the solvent. The arrow denotes the position of a methyne resonance which is partially obscured by a resonance of the residual aromatic protons of the toluene-d_8.

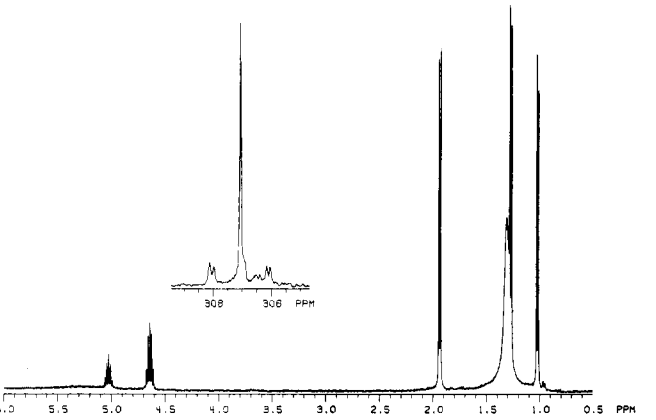

Figure 5. ^{1}H NMR spectrum of a sample of $[W_2(O\text{-}i\text{-}Pr)_6(\mu\text{-}CO)]_2$ dissolved in benzene-d_6, recorded at 360 MHz and 21 °C. The inset shows the ^{13}C NMR spectrum of the $[W_2(\mu\text{-}CO)]_2$ signal for a sample of $[W_2(O\text{-}i\text{-}Pr)_6(\mu\text{-}{}^*CO)]_2$ dissolved in toluene-d_8, where *C represents 92.5 atom % ^{13}C. The ^{13}C NMR spectrum was recorded at 90 MHz and 21 °C.

$Pr)_6(py)_2(\mu\text{-}CO)$" and an authentic sample of $[W_2(O\text{-}i\text{-}Pr)_6(py)(\mu\text{-}CO)]_2$ are the same except for the additional pyridine present in the former. Rather interestingly the chemical shift and the magnitude of $J_{^{183}W-^{13}C}$ are similar for the $W_2(\mu\text{-}CO)$ and $[W_2(\mu\text{-}CO)]_2$ moieties. A reexamination of the ^{13}C spectra recorded for "$W_2(O\text{-}i\text{-}Pr)_6(py)_2(\mu\text{-}{}^{13}CO)$" in benzene-$d_6$ (25.2 MHz, 34 °C) reveals precisely the spectrum reported for $[W_2(O\text{-}i\text{-}Pr)_6(py)(\mu\text{-}CO)]_2$ by Cotton and Schwotzer[6] in Table I of their paper. As noted in Table I, the magic angle spinning ^{13}C NMR chemical shift for $W_2(O\text{-}i\text{-}Pr)_6(py)_2(\mu\text{-}{}^{13}CO)$ in the solid state differs by 31 ppm from the solution value. These observations are, of course, consistent with our present finding that $W_2(O\text{-}i\text{-}Pr)_6(py)_2(\mu\text{-}CO)$ exists in the confacial bioctahedral geometry II only in the solid state and rapidly forms $[W_2(O\text{-}i\text{-}Pr)_6(\mu\text{-}CO)(py)]_2$ + 2py in toluene solutions.

During the course of this work which employed extensive use of $^{13}C{\equiv}O$ we were able to find bands in the IR spectrum at 1305 cm^{-1} for $[W_2(O\text{-}i\text{-}Pr)_6(py)(\mu\text{-}CO)]_2$ and at 1272 cm^{-1} for $[W_2(O\text{-}i\text{-}Pr)_6(\mu\text{-}CO)]_2$ which are associated with the central $[W_2(\mu\text{-}CO)]_2$ moiety. See Table I. These bands are probably predominantly ν(CO) in character.

The NMR spectra of the new compound $[W_2(O\text{-}i\text{-}Pr)_6(\mu\text{-}CO)]_2$ warrant special attention. As shown in Figure 4, at −75 °C samples of $[W_2(O\text{-}i\text{-}Pr)_6(\mu\text{-}CO)]_2$ in toluene-d_8 give a ^{1}H NMR spectrum that is consistent with the observed solid-state structure (Figure 2). The isopropoxy ligands give rise to six equally intense doublets in the region 0.8–2.2 ppm, two from the methyl groups of the O-*i*-Pr ligands that lie on the plane containing the $[W_2(\mu\text{-}CO)]_2$ unit and four from the diastereotopic methyl groups of the four terminal O-*i*-Pr ligands that lie off the plane. In addition there are four septets arising from the methyne protons with relative intensities 2:2:1:1. The two most intense septets are nearly degenerate, and another is partially obscured (the arrow points to it in Figure 4) by the resonance from the residual aromatic protons of the toluene-d_8 solvent.

As the temperature of the sample is raised from −75 to +60 °C, three of the doublets and two of the septets (one of intensity two and one of intensity one) broaden, coalesce, and sharpen to a single doublet and septet, respectively. The three remaining doublets and two of the septets remain sharp over the entire temperature range of −75 to +60 °C that we recorded spectra. These points are illustrated nicely by the room-temperature spectrum shown in Figure 5 where the three collapsed doublets appear as a broad resonance superimposed upon one of the sharp doublets and the collapsed septets appear as a broad roll in the base line at approximately 5.3 ppm.

$^{13}C\{^1H\}$ NMR spectra recorded at −55 and +20 °C, reported in the Experimental Section, complement the variable-temperature ^{1}H NMR results. Importantly, we observe two $^{183}W-^{13}C$ coupling constants for $[W_2(O\text{-}i\text{-}Pr)_6(^{13}CO)]_2$ at both −55 and +20 °C (see inset to Figure 6). This shows that the two tungsten atoms do not become equivalent on the NMR time scale at these temperatures.

We interpret the ^{1}H and ^{13}C NMR results in terms of a fluxional process involving scrambling of three O-*i*-Pr ligands, two of which lie off the mirror plane containing $[W_2(\mu\text{-}CO)]_2$ and one of which lies on the plane. The NMR experiments cannot distinguish which three O-*i*-Pr ligands are involved, but the most plausible exchange mechanism involves a pseudorotation of the three alkoxides attached to W(1). (See Figure 3).

Concluding Remarks

This work shows that the addition of 1 equiv of CO to $W_2(O\text{-}t\text{-}Bu)_6$ and $W_2(OCH_2\text{-}t\text{-}Bu)_6(py)_2$ leads to $W_2(O\text{-}t\text{-}Bu)_6(\mu\text{-}CO)$ and $W_2(OCH_2\text{-}t\text{-}Bu)_6(py)_2(\mu\text{-}CO)$, which adopt structures depicted by I and II, respectively, both in the solid state and in solution. While an analogous reaction leads to the isolation of $W_2(O\text{-}i\text{-}Pr)_6(py)_2(\mu\text{-}CO)$ as a microcrystalline precipitate from hexane, this compound is unstable with respect to loss of pyridine and "dimerization" to give the tetranuclear compound $[W_2(O\text{-}i\text{-}Pr)_6(py)(\mu\text{-}CO)]_2$. Cotton and Schwotzer's conclusion[6] concerning the position of the equilibrium shown in (2) is entirely correct and the ^{13}C NMR data reported for "$W_2(O\text{-}i\text{-}Pr)_6(py)_2(\mu\text{-}{}^{13}CO]$" by Chisholm and coworkers[3] are in fact due to $[W_2(O\text{-}i\text{-}Pr)_6(py)(\mu\text{-}{}^{13}CO)]_2$.

These observations are understandable in terms of steric control in the binding of pyridine and the nucleophilic properties of the $W_2(\mu\text{-}CO)$ oxygen atom. The bulky *tert*-butoxide ligands in $W_2(O\text{-}t\text{-}Bu)_6(\mu\text{-}CO)$ prevent both pyridine binding to the ditungsten center and its association to form a $[W_2(\mu\text{-}CO)]_2$ containing molecule supported by 12 O-*t*-Bu ligands. Addition of *i*-PrOH leads to *i*-PrO for *t*-BuO exchange and thus association to the tetranuclear compound $[W_2(O\text{-}i\text{-}Pr)_6(\mu\text{-}CO)]_2$ becomes possible on steric grounds. The neopentoxy ligands are less sterically demanding than either *t*-BuO or *i*-PrO ligands and Lewis

bases are known to bind to $W_2(OR)_6L_2$ compounds in the order R = CH_2-*t*-Bu > *i*-Pr > *t*-Bu.[7] Consequently, the $W_2(OCH_2$-*t*-$Bu)_6(py)_2(\mu$-CO) molecule can accommodate both pyridine ligands which prevents formation of the $[W_2(\mu$-CO)$]_2$ containing compound supported by neopentoxide ligands. The *i*-PrO ligands which are intermediate with respect to pyridine binding forms $W_2(O$-*i*-$Pr)_6(py)_2(\mu$-CO) as the kinetic product in hexane solution. This is only isolated because of its low solubility in hexane. In toluene solution $[W_2(O$-*i*-$Pr)_6(py)(\mu$-CO)$]_2$ is formed according to eq 2.

At this point it is worth asking: what evidence is there for the cleavage of the tetranuclear $[W_2(\mu$-CO)$]_2$-containing compounds to regenerate dinuclear $W_2(\mu$-CO)-containing compounds. We have found that they are not cleaved by pyridine or PMe_3 which indicate that the equilibrium in (2) lies well to the right. Addition of C_2H_2 (>2 equiv) leads to the formation of $W_2(O$-*i*-$Pr)_6(\mu$-$C_4H_4)$(CO) which shows that a terminal C≡O ligand can be generated from the $[W_2(\mu$-CO)$]_2$ unit. However, the details of this and other reactions involving the μ-CO ligands in these compounds are currently under investigation and will be reported subsequently.

Finally we note that CO binds more strongly to the $(W{\equiv}W)^{6+}$ center than it does to the $(Mo{\equiv}Mo)^{6+}$ center and that the reaction sequence W≡W + C≡O → $W_2(\mu$-CO) → $[W_2(\mu$-CO)$]_2$, which involves the stepwise reduction of M–M and C–O bond orders from 3 → 2 → 1, is suggestive of a model for the reductive cleavage of C≡O to carbide, C^{4-}, and oxide, O^{2-}, ligands, on a metal oxide. This is believed to be a fundamental step in Fischer–Tropsch chemistry, where CO and H_2 mixtures are converted to a broad range of products including alkanes, alkenes, and water. Cleavage of the C–O bond of a carbonyl ligand in metal carbonyl clusters has been reported recently by using HSO_3CF_3 as a proton source.[10] Further studies of the reaction chemistry of these $W_2(\mu$-CO)- and $[W_2(\mu$-CO$)]_2$-containing compounds are clearly warranted.

Experimental Section

Reagents and General Techniques. General procedures and the preparations of $W_2(OR)_6(py)_2$, R = *i*-Pr and CH_2-*t*-Bu, and $W_2(O$-*t*-$Bu)_6$ have been described.[11] Dry and oxygen-free hexanes, toluene, and pyridine were used in all preparations.

^{1}H NMR spectra were recorded on a Nicolet NT-360 360-MHz spectrometer using dry and oxygen-free toluene-d_8 or benzene-d_6. ^{13}C NMR spectra were recorded on the same instrument at 90 MHz. All ^{1}H NMR chemical shifts are in parts per million relative to the CHD_2 quintet of toluene-d_8 set at δ 2.09 or the residual protons of benzene-d_6 set at δ 7.15. ^{13}C NMR chemical shifts are reported in parts per million relative to the ipso carbon of the toluene-d_8 solvent set at δ 137.5 or relative to the aromatic carbon atoms of benzene-d_6 set at δ 128.0. All ^{13}C NMR spectra were recorded for the ^{13}CO-labeled complexes.

Infrared spectra were obtained on a Perkin-Elmer 283 spectrophotometer as Nujol mulls between CsI plates unless otherwise noted. Elemental Analyses were performed by Bernhardt Analytical Laboratories of West Germany.

$W_2(O$-*t*-$Bu)_6(\mu$-CO). In a Schlenk reaction flask, equipped with a tight fitting septum, $W_2(O$-*t*-$Bu)_6$ (0.90 g, 1.1 mmol) was dissolved in hexane (12 mL). The flask was closed to nitrogen flow and then cooled to 0 °C. Carbon monoxide (1.1 mmol), drawn from a calibrated vacuum manifold with a 10-cm^3 gas-tight syringe, was then injected through the septum. Immediately a red solid began to precipitate from solution. The reaction mixture was stirred at 0 °C for 1 h and then placed in a freezer at −15 °C for 2 h. This produced red microcrystals which were collected by filtration and dried in vacuo (yield 0.64 g, 68%). X-ray crystallographic quality crystals were grown from toluene solutions. Anal. Calcd for $W_2O_7C_{25}H_{54}$: C, 35.99; H, 6.52. Found: C, 35.89; H, 6.18.

^{1}H NMR (21 °C, benzene-d_6): δ(OC*Me*$_3$) 1.45. ^{13}C{^{1}H} NMR (21 °C, benzene-d_6): δ(CO) 291.0 (J_{WC} = 192.9 Hz); δ(OC*Me*$_3$) 32.6; δ(O*C*Me$_3$) 83.6. IR (cm^{-1}): ν_{CO} 1598 s ($\nu_{^{13}CO}$ = 1559), 1335 m, 1170 s, 1024 m, 972 vs, 923 s, 886 m, 785 m, 778 m, 581 m, 561 m, 523 m, 503 w, 475 w, 460 m, 360 m, 263 w. IR (Cm^{-1}, toluene): ν_{CO} 1605.

$W_2(OCH_2$-*t*-$Bu)_6(py)_2(\mu$-CO). This complex was prepared from $W_2(OCH_2$-*t*-$Bu)_6(py)_2$ by a procedure analogous to that described for $W_2(O$-*t*-$Bu)_6(\mu$-CO). It is isolated as a brown powder from hexane or pentane solutions (yield 78%). A satisfactory analysis was not obtained. Anal. Calcd for $W_2O_7N_2C_{41}H_{76}$: C, 45.73; H, 7.11; N, 2.60. Found: C, 40.91; H, 6.37; N, 2.26.

^{1}H NMR (−60 °C, toluene-d_8): δ(OCH$_2$-t-*Bu*) 0.97 (18 H, s), 1.26 (36 H, s); δ(OC*H*$_2$-*t*-Bu) 3.72 (4 H, s), 4.11 (4 H, d of an AB q, J_{HH} = 10.1 Hz), 5.49 (4 H, d of an AB q, J_{HH} = 10.1 Hz); δ(py) 6.65 (4 H, t), 6.76 (2H, t), and 9.47 (4 H, d). ^{13}C{^{1}H} NMR (−60 °C, toluene-d_8): δ(CO) 321.6 (J_{WC} = 150.3 Hz), δ(OCH$_2$C*Me*$_3$) 27.4, 27.7; δ(OCH$_2$*C*Me$_3$) 34.9, 35.2; δ-(O*C*H$_2$CMe$_3$) 89.5, 88.3. IR (cm^{-1}): ν_{CO} 1587, 1579, 1567 s ($\nu_{^{13}CO}$ 1546, 1538), 1601 s, 1391 s, 1290 w, 1257 w, 1235 vw, 1217 m, 1152 w, 1146 w, 1058 s, 1015 s, 932 w, 902 w, 760 m, 755 s, 698 s, 665 s, 649 s, 621 m, 593 w, 575 w, 514 vw, 452 m, 432 w, 404 m, 330 m, 283 w. IR (cm^{-1}, toluene): ν_{CO} 1595 ($\nu_{^{13}CO}$ 1570).

$W_2(O$-*i*-$Pr)_6(py)_2(\mu$-CO). This compound is easily prepared from $W_2(O$-*i*-$Pr)_6(py)_2$ by a procedure analogous to that described for $W_2(O$-*t*-$Bu)_6(\mu$-CO). It is isolated as a golden brown powder from hexanes solutions (yield 83%). Crystals suitable for X-ray crystallography can be obtained from the reaction solution if a solvent mixture of hexanes/pyridine is used (6 mL/1 mL).

^{1}H NMR (21 °C, toluene-d_8): δ(OCH*Me*$_2$) 1.11, 1.21, 1.79 (12 H, d, J_{HH} = 6 Hz), 1.26 (36 H, br), δ(OC*H*Me$_2$) 4.39 (4 H), 5.17 (2 H) (sept, J_{HH} = 6 Hz), 5.2 (6 H, v br); δ(py) 6.75 (8 H, t), 7.03 (4 H, t), 8.77 (8 H, d). See $[W_2(O$-*i*-$Pr)_6(py)(CO)]_2$ for comparison. IR (cm^{-1}): ν_{CO} 1579, 1570 s ($\nu_{^{13}CO}$ 1533), 1602 m, 1534 w, 1486 m, 1332 m, 1327 m, 1311 m, 1237 vw, 1219 m, 1165 m, 1158 m, 1118 s, 1074 m, 1040 m, 1013 m, 994 s, 982 s, 959 s, 942 s, 848 m, 838 m, 754 m, 699 m, 649, vw, 638 m, 614 m, 606 s, 570 w, 538 w, 508 vw, 451 w, 435 w, 312 m. IR (cm^{-1}, toluene): ν_{CO} 1298 ($\nu_{^{13}CO}$ 1271).

$[W_2(O$-*i*-$Pr)_6(py)(CO)]_2$. $W_2(O$-*i*-$Pr)_6(py)_2(\mu$-CO) quantitatively converts to $[W_2(O$-*i*-$Pr)_6(py)(CO)]_2$ + 2 py in toluene or benzene. Red crystals of $[W_2(O$-*i*-$Pr)_6(py)(CO)]_2$ can be isolated from toluene solutions (yield 65%).

^{1}H NMR (−60 °C, toluene-d_8): δ(OCH*Me*$_2$) 1.12, 1.35, 1.44, 1.76 (12 H, d, J_{HH} = 5 Hz), 1.29 (overlapping d); δ(OC*H*Me$_2$) 4.38 (2 H), 4.93 (2 H), 5.23 (4 H), 6.35 (4 H) (br sept); δ(py) 6.86 (4 H, br), 7.10 (2 H, br), 9.74 (4 H, br); (21 °C, toluene-d_8) δ(OCH*Me*$_2$) 1.11 1.20, 1.78 (12 H, d, J_{HH} = 6 Hz), 1.26 (36 H, br d); δ(OC*H*Me$_2$) 4.38 (4 H), 5.18 (2 H) sept, J_{HH} = 6 Hz), 5.2 (6 H, v br); δ(py) 6.85 (4 H, t), 7.11 (2 H, t), 9.32 (4 H, d). IR (cm^{-1}): ν_{CO} 1305 s ($\nu_{^{13}CO}$ 1265), 1598 m, 1571 w, 1515 w, 1323 s, 1230 vw, 1209 s, 1160 s, 1117 s, 1069 m, 1032 m, 980 s, 955 s, 846 s, 760 m, 751 m, 692 s, 641 s, 606 s, 585 s, 494 m, 460 s, 451 s, 429 m, 370 w, 305 m, 281 m. IR (cm^{-1}, toluene): ν_{CO} 1298.

$[W_2(O$-*i*-$Pr)_6(CO)]_2$. Two procedures resulted in the preparation of this compound: (a) To $W_2(O$-*t*-$Bu)_6(\mu$-CO) (0.64 g, 0.77 mmol) was added *i*-PrOH(10 mL). The resulting red solution was stirred at room temperature for 4 h. The volume was then reduced and the solution warmed slightly (40–50 °C) to dissolve some precipitate that had formed. Cooling at −15 °C for 24 h resulted in red microcrystals that were isolated by filtration and dried in vacuo (yield 0.30 g, 52%). ^{1}H NMR spectra of stripped reaction mixtures revealed virtually quantitative formation of the W_4 species. (b) To $W_2(O$-*i*-$Pr)_6(PMe_3)_2$ (0.40 g, 0.46 mmol) dissolved in hexane (8 ml), cooled to 0 °C, was added CO (0.46 mmol) via a gas-tight syringe. The reaction mixture was stirred for 1 h at 0 °C, and then the volatiles were removed. The residue was redissolved in warm (40–50 °C) *i*-PrOH. Cooling at −15 °C for 3 days produced red crystals (yield 0.09 g, 26%). Anal. Calcd for $W_4O_{14}C_{38}H_{84}$: C, 30.42; H, 5.64. Found: C, 30.21; H, 5.60.

^{1}H NMR (−80 °C, toluene-d_8): δ (OCH*Me*$_2$) 1.02, 1.09, 1.21, 1.31, 1.72, 1.94 (12 H, d, J_{HH} = 6 Hz); δ(OC*H*Me$_2$) 4.67 (8 H,

(10) Drezdzon, M. A.; Whitmire, K. H.; Bhattacharyya, A. A.; Wen-Liang, H.; Nagel, C. C.; Shore, S. G.; Shriver, D. F. *J. Am. Chem. Soc.* **1982**, *104*, 5630 and references therein.

(11) Akiyama, M.; Chisholm, M. H.; Cotton, F. A.; Extine, M. W.; Haitko, D. A.; Little, D.; Fanwick, P. E. *Inorg. Chem.* **1979**, *18*, 2321.

Table VII. Crystal Data Summary[a]

	I	II
empirical formula	$W_2C_{25}H_{54}O_7$	$W_4C_{38}H_{84}O_{14}$
color of cryst	black	black (red)
cryst dimens, mm	0.04 × 0.05 × 0.10	0.04 × 0.08 × 0.15
space group	$Cmc2_1$	$P2_1/n$
cell dimens		
temp, °C	−162	−162
a, Å	17.669 (2)	12.085 (2)
b, Å	9.182 (13)	17.224 (4)
c, Å	19.307 (5)	13.027 (3)
β		99.25 (1)
Z (molecules/cell)	4	2
vol, Å^3	6261.42	2676.36
d(calcd), g/cm^3	1.770	1.862
wavelength, Å	0.710 69	0.710 69
mol wt	834.40	1500.47
linear abs coeff, cm^{-1}	75.361	88.029
max absorptn		0.4890
min absorptn		0.7660
detector to sample dist, cm	22.5	22.5
sample to source dist, cm	23.5	23.5
av *ω* scan width at half height	0.25	0.25
scan speed, deg/min	4.0	4.0
scan width, deg + dispersn	2.0	2.0
individual bkgd, s	6	8
aperture size, mm	3.4 × 4.0	3.0 × 4.0
2*θ* range, deg	6–45	6–45
total no. of reflctns collected	6360	3941
no. of unique intensities	1105	3513
no. of $F > 3.00\sigma(F)$	1072	3105
$R(F)$	0.0310	0.0406
$R_w(F)$	0.0347	0.0410
goodness of fit for the last cycle	1.105	1.134
max δ/σ for last cycle	0.05	0.08

[a] I = W_2(O-*t*-Bu)$_6$(*μ*-CO); II = [W_2(O-*i*-Pr)$_6$(*μ*-CO)]$_2$.

overlapping sept, J_{HH} = 6 Hz), 4.92 (2 H, br sept), 6.98 (2 H, br sept); (21 °C, toluene-d_8) δ(OCH*Me*$_2$) 1.02, 1.27, 1.93 (12 H, d, J_{HH} = 6 Hz), 1.31 (36 H, br); δ(OC*H*Me$_2$) 4.64 (4 H), 5.02 (2 H) (sept, J_{HH} = 6 Hz), 5.3 (6 H, v br). $^{13}C\{^1H\}$ NMR (−55 °C, toluene-d_8): δ(CO) 305.5 (J_{W_1C} = 164.0 and J_{W_2C} = 188.9 Hz); δ(OCH*Me*$_2$) 25.1 (4 C), 26.4 (4 C), 26.9 (4 C), 27.4 (4 C) 26.7 (8 C); δ(O*C*HMe$_2$) 75.6 (4 C), 76.2 (4 C), 76.4 (2 C), 80.2 (2 C); (20 °C, toluene-d_8) δ(CO) 307.0 (J_{W_1C} = 164.7 and J_{W_2C} = 189.0 Hz); δ(OCH*Me*$_2$) 25.1 (4 C), 26.4 (4 C), 27.3 (4 C), 26.8 (12 C); δ(O*C*HMe$_2$) 75.9 (10 C), 80.8 (2 C). IR (cm^{-1}): ν_{CO} 1272 s ($\nu_{^{13}CO}$ 1243), 1331 m, 1323 m, 1166 s, 1116 s, 985 s, 951 s, 849 s, 658 m, 600 s, 545 w, 453 m, 423 w, 317 w, 293 w.

Crystallographic Studies. General operating procedures and listings of programs have been previously reported.[12] Crystal data for W_2(O-*t*-Bu)$_6$(*μ*-CO) and [W_2(O-*i*-Pr)$_6$(*μ*-CO)]$_2$ are summarized in Table VII.

[W_2(O-*i*-Pr)$_6$(*μ*-CO)]$_2$. A suitable sample was obtained by cleaving a larger crystal in a nitrogen-filled glovebag and transferring the sample to the goniostat where it was cooled to −162 °C. A systematic search of a limited hemisphere of reciprocal space located diffraction mamima which could be indexed as monoclinic of space group $P2_1/n$.

Data were collected in the usual manner and the structure solved by a combination of direct methods, Patterson techniques, and Fourier techniques, *ψ* scans of several reflections indicated the necessity of an absorption correction. Although the fragment was not well-formed, it was possible to assign indicies to the faces for the analytical correction. The error for equivalent data was reduced from 0.165 to 0.054 after correction, and the residuals were reduced by about 50%. Hydrogen atoms were clearly visible in a difference Fourier phased on the refined non-hydrogen positions and were included in the final refinement. It should be noted that several of the hydrogens are poorly determined (see thermal parameters, distances and angles) although they are qualitatively correct.

One interesting note is that in the early stages of refinement, it was noted that O(1) and C(1) thermal parameters were such that one could suspect some "scrambling". In general the thermal parameters of C(1) was consistently low while that of O(1) was relatively large. To confirm that no scrambling was present, the occupancies of each were varied, allowing a fraction *X* for one element and 1 − X for the other. The resulting refinement indicated 98% O for O(1) and 99% C for C(1). This implies that the low thermal parameters for C(1) are in fact due to it being held rather "rigidly" by the two tungsten atoms and O(1).

W_2(O-*t*-Bu)$_6$(*μ*-CO). A suitable crystal was transferred to the goniostat as described above and cooled to −162 °C. Examination of a limited hemisphere of reciprocal space revealed a set of strong diffraction maxima corresponding to a cell isomorphous to that of Mo_2(O-*t*-Bu)$_6$(*μ*-CO), with only slightly different cell parameters. It was also discovered that the streaking noticed in the Mo structure was present and in fact corresponded to a well-defined primitive cell double along *a*. Examination of several other crystals from different crystalizations and at different temperatures indicated that the weak diffractions were more pronounced at lower temperatures (as would be expected) and that the relative intensities of the weak reflections compared to the stronger reflections varied from crystal to crystal. This phenomenon is characteristic of "order–disorder structures" as described by K. Dornberger-Schiff [*Acta Crystallogr.* **1956**, *9*, 593–601]. For this reason, the weak intensities were rejected and the structure was solved and refined in space group $Cmc2_1$, that reported for M = Mo. The W and O atoms as well as the carbonyl C atom were refined anisotropically by full-matrix least squares using fixed idealized hydrogen contributors. A final difference Fourier was featureless, the largest peak being 0.38 e/Å^3. *ψ* scans of several reflections were essentially flat, and no absorption correction was performed.

Acknowledgment. We thank the donors of the Petroleum Research Fund administered by the American Chemical Society, the Department of Energy, Office of Basic Research, Chemical Sciences Division and the Wrubel Computing Center at Indiana University for support.

Registry No. I (M = W, R = *t*-Bu), 95674-36-5; II (M = W, R = CH$_2$-*t*-Bu), 95674-37-6; II (M = W, R = *i*-Pr), 83436-99-1; VI (M = W, R = *i*-Pr), 85956-37-2; [W_2(O-*i*-Pr)$_6$(*μ*-CO)]$_2$, 95674-38-7; W_2(O-*t*-Bu)$_6$, 57125-20-9; W_2(OCH$_2$-*t*-Bu)$_6$(py)$_2$, 88608-50-8; W_2(O-*i*-Pr)$_6$(py)$_2$, 70178-75-5; W_2(O-*i*-Pr)$_6$(PMe$_3$)$_2$, 84028-41-1; W, 7440-33-7.

Supplementary Material Available: Tables of observed and calculated structure factors, anisotropic thermal parameters, complete listings of bond length and bond angles, deviation of atoms from least-squares planes for the [W_2(O)$_6$(*μ*-CO)]$_2$ units in [W_2(O-*i*-Pr)$_6$(py)(*μ*-CO)]$_2$ and [W_2(O-*i*-Pr)$_6$(*μ*-CO)]$_2$ (46 pages). Ordering information is given on any current masthead page. The complete structure reports are available from Indiana University Library in microfiche form only, at a cost of $2.50 per report. For W_2(O-*t*-Bu)$_6$(*μ*-CO) request MSC Report No. 84006 and for [W_2(O-*i*-Pr)$_6$(*μ*-CO)]$_2$, MSC Report No. 84012.

(12) Chisholm, M. H.; Folting, K.; Huffman, J. C.; Kirkpatrick, C. C. *Inorg. Chem.* **1984**, *23*, 1021.